Electronic Supplementary Material (ESI) for Physical Chemistry Chemical Physics.
This journal is © the Owner Societies 2014

Supplementary information for ”H_2 production through electro-oxidation of SO_2: identifying the fundamental limitations”

Roelof J. Kriek,[a] Jan Rossmeisl,[b] Samira Siahrostami[b] and Mårten E. Björketun[b]

PGM Group, Research Focus Area for Chemical Resource Beneficiation (CRB), North-West University, Potchefstroom 2520, South Africa.

Center for Atomic-scale Materials Design (CAMD), Department of Physics, Technical University of Denmark, DK-2800 Lyngby, Denmark.

1 Reaction free energies along Path 1

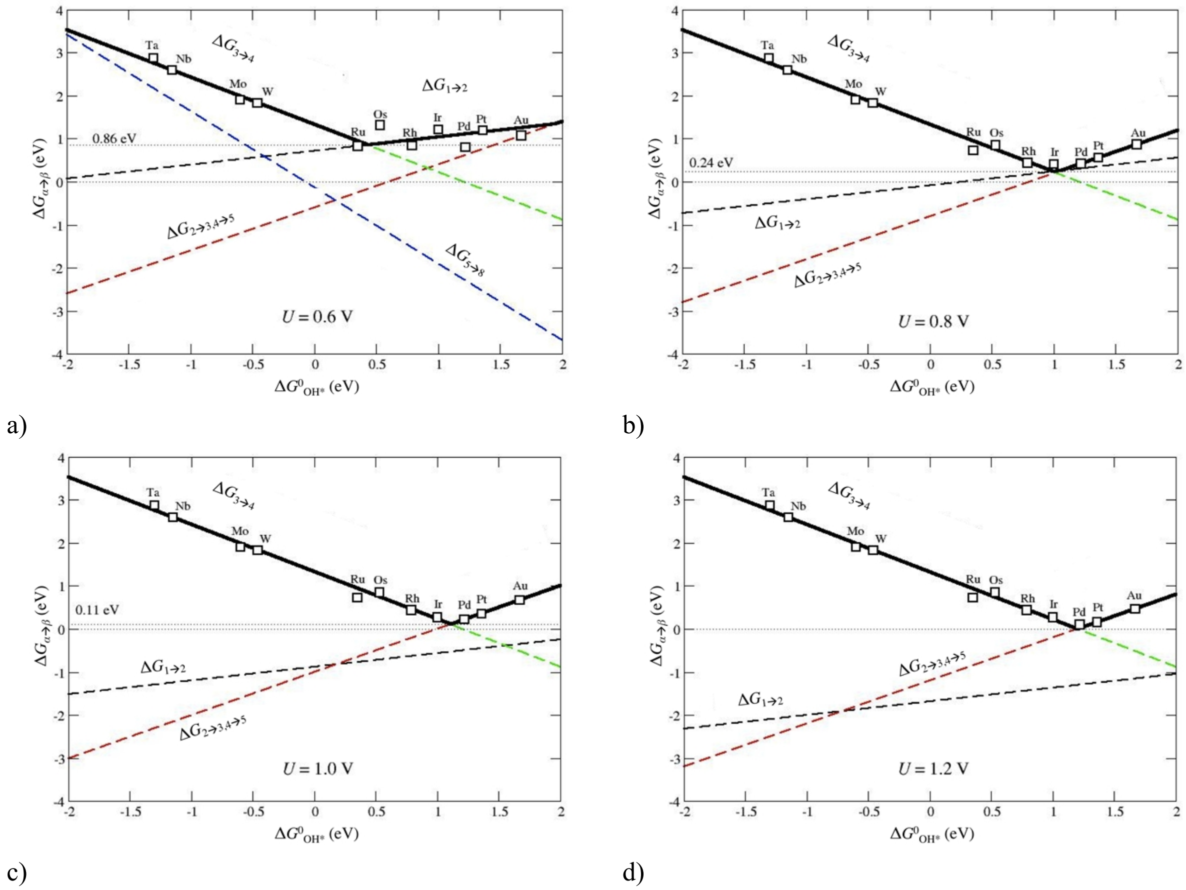

Figure S1: Reaction free energy of the elementary steps along Path 1 as a function of ΔG^0_{OH*} at (a) $U = 0.6$ V, (b) $U = 0.8$ V, (c) $U = 1.0$ V and (d) $U = 1.2$ V on the RHE scale. The free energy of the limiting step(s) is indicated with a solid black line. Dashed lines are reaction free energies estimated from the linear correlations in Fig. 3 (their functional forms are given by Eqs. S14-S18), whereas squares indicate the maximum reaction free energy encountered along the reaction path for individual metals. The chemical step 5→8 is excluded from plots (b)-(d) since it is always considerably more facile than the chemical step 3→4.

We first investigate the energetics of Path 1, the HSO_3 intermediate reaction pathway. In Figure S1 we report the reaction free energies, $\Delta G_{\alpha\rightarrow\beta}$, of the elementary steps in Path 1 as a function of ΔG^0_{OH*} at four different potentials, U = 0.6, 0.8, 1.0 and 1.2 V vs RHE. The results and conclusions are very similar to those we obtained for Path 2 in the main paper. As for Path 2, a high chemical barrier, this time 3→4, will disqualify reactive metals as SO_2 electro-oxidation catalysts despite the facile oxidation of S* to SO_2 and adsorption of OH*. Again, a much higher activity can be obtained on less active metals but at the cost of running the reaction at high overpotentials. The only difference compared with Path 2 is that slightly more reactive metals (with OH* binding similar to Pd instead of Pt) will be the best candidates. This time Pd is the least noble metal on which each elementary step along the reaction pathway can be made exergonic.

2 Kinetic modelling

We then construct a simple kinetic model for sulphur oxidation along Path 1

$S^* + 4H_2O(l)$ ☒ $SO_2^* + 2H_2O(l) + 2H_2(g)$ ☒ $SO_2^* + OH^* + H_2O(l) + 5/2H_2(g)$ ☒

$HSO_3^* + H_2O(l) + 5/2H_2(g)$ ☒ $HSO_3^* + OH^* + 3H_2(g)$ ☒ $H_2SO_4(l) + 3H_2(g)$ (S1)

and Path 2

$S^* + 4H_2O(l)$ ☒ $SO_2^* + 2H_2O(l) + 2H_2(g)$ ☒ $SO_2^* + OH^* + H_2O(l) + 5/2H_2(g)$ ☒

$SO_2^* + O^* + H_2O(l) + 3H_2(g)$ ☒ $SO_3^* + H_2O(l) + 3H_2(g)$ ☒ $H_2SO_4(l) + 3H_2(g)$ (S2)

To start with we derive expressions for the reaction free energies along the two pathways. The free energies of the reaction intermediates and the product $H_2SO_4(l)$ have been calculated relative to $SO_2(g)$, $H_2O(l)$ and $H^+(aq)+e^-$ pairs, assuming standard conditions. Using the scaling relations reported in Fig. 3, they can be written as a function of both $\Delta G^0_{OH*} = \Delta G_{OH*}(U{=}0)$ and U, resulting in (Path 1)

$\Delta G_{S*} = 0.55\cdot\Delta G^0_{OH*} - 4.00 + 4U$ (S3)

$\Delta G_{SO2*} = 0.87\cdot\Delta G^0_{OH*} - 0.88 + 0U$ (S4)

$\Delta G_{OH*} = 1.00\cdot\Delta G^0_{OH*} + 0.00 - 1U$ (S5)

$\Delta G_{HSO3*} = 0.77\cdot\Delta G^0_{OH*} + 0.45 - 1U$ (S6)

$\Delta G_{H2SO4(l)} = 0.32 - 2U$ (S7)

and (Path 2)

$\Delta G_{S*} = 0.55\cdot\Delta G^0_{OH*} - 4.00 + 4U$ (S8)

$\Delta G_{SO2*} = 0.87\cdot\Delta G^0_{OH*} - 0.88 + 0U$ (S9)

$\Delta G_{OH*} = 1.00\cdot\Delta G^0_{OH*} + 0.00 - 1U$ (S10)

$\Delta G_{O*} = 1.51\cdot\Delta G^0_{OH*} - 0.56 - 2U$ (S11)

$\Delta G_{SO3*} = 1.26\cdot\Delta G^0_{OH*} + 0.06 - 2U$ (S12)

$\Delta G_{H2SO4(l)} = 0.32 - 2U$ (S13)

By combining these relations we then obtain expressions for the reaction free energies of the various steps along Path 1

$$\Delta G_{1\rightarrow 2} = \Delta G_{SO2*} - \Delta G_{S*} = 0.32\cdot\Delta G^{0}_{OH*} + 3.12 - 4U \tag{S14}$$

$$\Delta G_{2\rightarrow 3} = \Delta G_{OH*} = 1.00\cdot\Delta G^{0}_{OH*} + 0.00 - 1U \tag{S15}$$

$$\Delta G_{3\rightarrow 4} = \Delta G_{HSO3*} - (\Delta G_{SO2*} + \Delta G_{OH*}) = -1.10\cdot\Delta G^{0}_{OH*} + 1.33 \tag{S16}$$

$$\Delta G_{4\rightarrow 5} = \Delta G_{2\rightarrow 3} = 1.00\cdot\Delta G^{0}_{OH*} + 0.00 - 1U \tag{S17}$$

$$\Delta G_{5\rightarrow 8} = \Delta G_{H2SO4(l)} - \Delta G_{HSO3*} - \Delta G_{OH*} = -1.77\cdot\Delta G^{0}_{OH*} - 0.13 \tag{S18}$$

and Path 2

$$\Delta G_{1\rightarrow 2} = \Delta G_{SO2*} - \Delta G_{S*} = 0.32\cdot\Delta G^{0}_{OH*} + 3.12 - 4U \tag{S19}$$

$$\Delta G_{2\rightarrow 3} = \Delta G_{OH*} = 1.00\cdot\Delta G^{0}_{OH*} + 0.00 - 1U \tag{S20}$$

$$\Delta G_{3\rightarrow 6} = \Delta G_{O*} - \Delta G_{OH*} = 0.51\cdot\Delta G^{0}_{OH*} - 0.56 - 1U \tag{S21}$$

$$\Delta G_{6\rightarrow 7} = \Delta G_{SO3*} - \Delta G_{SO2*} - \Delta G_{O*} = -1.12\cdot\Delta G^{0}_{OH*} + 1.50 \tag{S22}$$

$$\Delta G_{7\rightarrow 8} = \Delta G_{H2SO4(l)} - \Delta G_{SO3*} = -1.26\cdot\Delta G^{0}_{OH*} + 0.26 \tag{S23}$$

The kinetic model takes Eqs. S14-S18 and S19-S23 as input and uses them as estimates of the free energy barriers encountered along Path 1 and Path 2, respectively. Accordingly, extra barriers on top of the reaction free energies are ignored. In addition, we neglect potential coverage effects. The calculated oxidation rates should thus be viewed as upper bounds. For a given U, the model gives as output the maximum oxidation rate that can be obtained on any close-packed transition metal surface. It determines this maximum rate by first identifying the limiting step (highest $\Delta G_{\alpha\rightarrow\beta}$) as a function of ΔG^{0}_{OH*}[1] and then minimizing the limiting barrier with respect to ΔG^{0}_{OH*}. The whole procedure can be expressed in compact mathematical form; as

(S24)

for Path 1 and as

(S25)

for Path 2. It is important to note that this model is unable to predict drops in activity at higher potentials due to, for instance, oxidation of the surface; once the activity has reached its maximum it will stay the same indefinitely.

Figure S2 shows the potential-dependent activities as obtained with these expressions (solid lines). Moreover, it reports the maximum activities and the potential at which they are reached for a set of close-packed transition metal surfaces. Figure S2 suggests that by employing increasingly noble catalysts, the activity can be steadily increased for potentials up to ~1.2 V vs RHE along Path 1 and up

---

[1] ΔG^{0}_{OH*} is a measure of the surface reactivity and can be varied continuously. It can thus be considered a meta-material parameter.

to ~1.35 V vs RHE along Path 2.

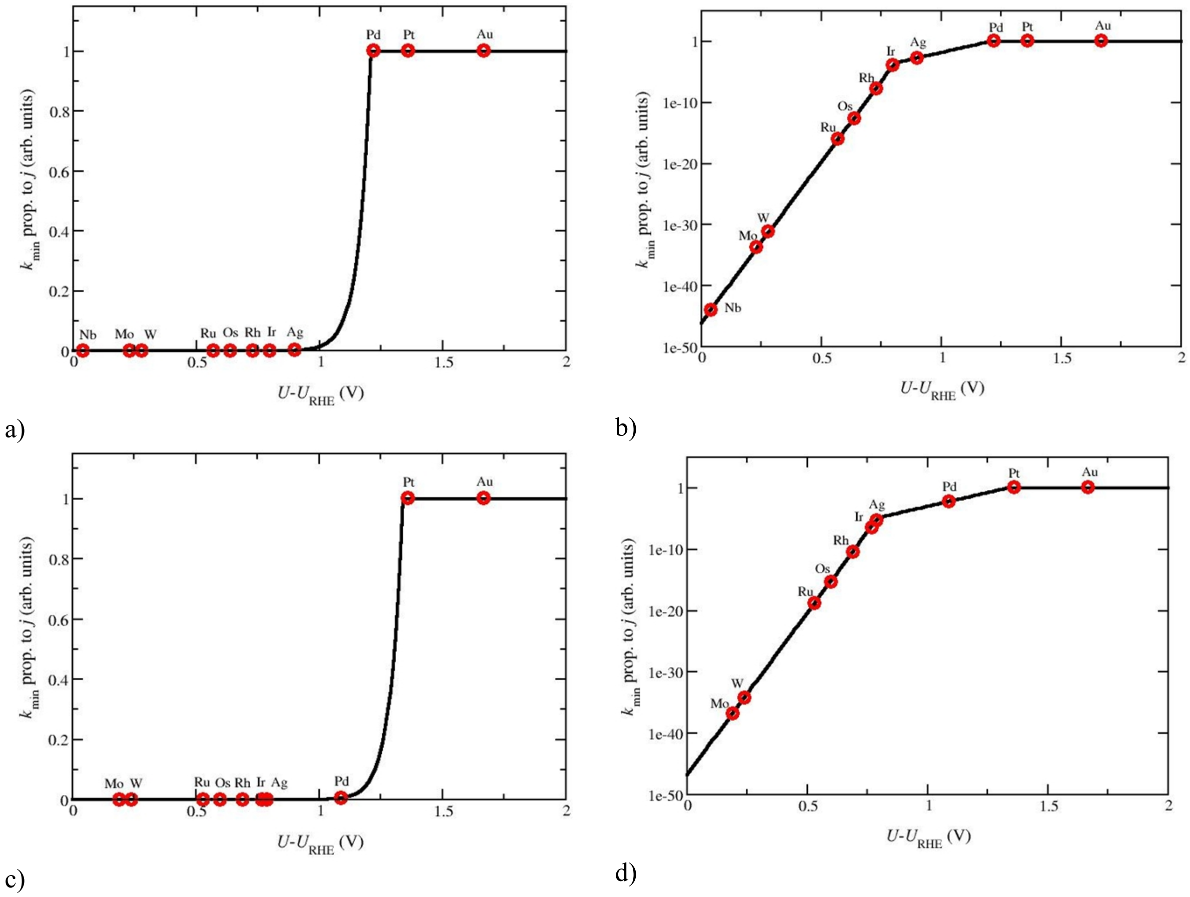

a)

b)

c)

d)

Figure S2: Normalized maximum achievable SO_2 oxidation rate as a function of electrode potential (solid line) for Path 1 (a,b) and Path 2 (c,d): (a,c) linear scale and (b,d) logarithmic scale. Circles indicate the maximum catalytic activities of specific close-packed transition metal surfaces and the potentials at which they are obtained.

2.1 Solvent effects

Equations S3-S23 were derived based on DFT data obtained on systems without solvent. This means we have not accounted for the potential stabilization (or destabilization) of adsorbates by electrolyte molecules, in particular water molecules, and its impact on the reaction free energies (S14-S23). The effect of solvent will be biggest for reaction steps involving OH*, i.e. for steps 2→3 and 3→6 in the case of Path 2, since OH is the molecule most prone to form strong hydrogen bonds with the surrounding water molecules. The minor changes in $\Delta G_{1\rightarrow 2}$, $\Delta G_{6\rightarrow 7}$ and $\Delta G_{7\rightarrow 8}$ that might arise from the introduction of a solvent are not expected to affect any of the previous results and conclusions. In the following we will demonstrate that stabilization of OH* also has a rather limited effect on the overall picture – except for a lowering of the peak potential of noble metals nothing changes.

First of all, we note that the water induced OH* stabilization will not influence the maximum catalytic rate and peak potential of the more reactive metals as the oxidation on these metals is limited by step 6→7. From earlier DFT based work on Pt(111)[1] we know that a bilayer of water stabilizes OH* with ~0.6 eV, a value we will use for all metals except Ag. Contrary to Pt(111) where the preferred adsorption site for OH is atop Pt both without and in the presence of water, the preferred adsorption site on Ag(111) changes from fcc to atop when water is introduced, and this reduces the water induced stabilization to ~0.1 eV. We take all these considerations into account and modify the kinetic model for Path 2 accordingly. The result is reported in Figure S3. Comparison with the previous result for Path 2 (Figure S2 c,d) shows that while nothing changes for the reactive metals, the peak potential has been lowered ~0.45 V on the more noble metals and the activity can now be steadily increased (by employing increasingly noble catalysts) for potentials up to ~0.9 V instead of ~1.35 V vs RHE. Moreover, as a result of the relatively small OH* stabilization, Ag has now become a more interesting candidate. For similar reasons, though that has not been considered here, Pd would be somewhat more active than any of the plots suggests.

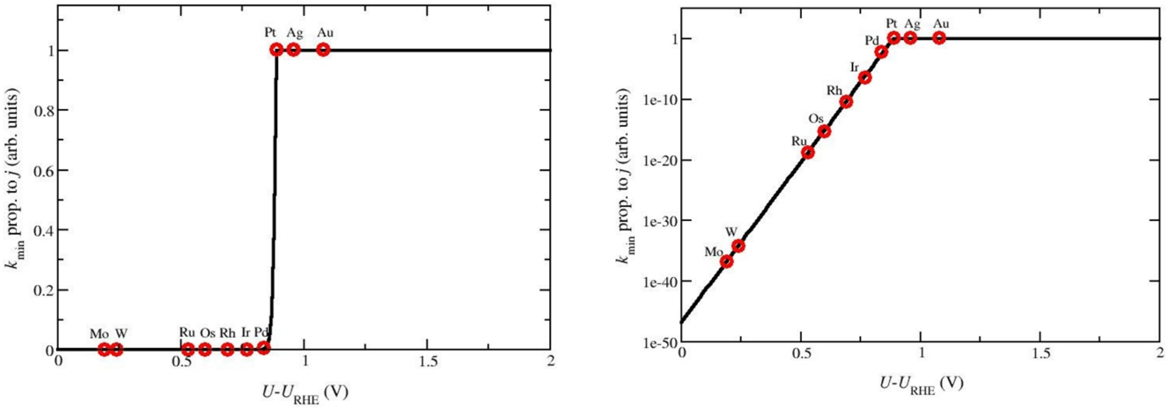

a)

b)

Figure S3: Normalized maximum achievable SO_2 oxidation rate as a function of electrode potential (solid line) for Path 2 when stabilization of OH* by water is taken into account: a) linear scale and b) logarithmic scale.

References

---

[1] J. Rossmeisl, J. K. Nørskov, C. D. Taylor, M. J. Janik and M. Neurock, *J. Phys. Chem. B*, 2006, **110**, 21833.